Design Considerations for an Integrated Solar Sail Diagnostics System

Christopher H. M. Jenkins* and Aaron R. Gough†
South Dakota School of Mines and Technology, Rapid City, South Dakota 57701

Richard S. Pappa‡
NASA Langley Research Center, Hampton, Virginia 23681

Joe Carroll§
Tether Applications, Inc., Chula Vista, California 91913

Joseph R. Blandino** and Jonathan J. Miles††
James Madison University, Harrisonburg, Virginia 22807

and

John Rakoczy‡‡
NASA Marshall Space Flight Center, Huntsville, Alabama 35812

Efforts are continuing under NASA support to improve the readiness level of solar sail technology. Solar sails have one of the best chances to be the next gossamer spacecraft flown in space. In the gossamer spacecraft community thus far, solar sails have always been considered a "low precision" application compared with, say, radar or optical devices. However, as this paper shows, even low precision gossamer applications put extraordinary demands on structural measurement systems if they are to be traceable to use in space.

I. Introduction

NASA's new In-Space Propulsion (ISP) program recently selected teams led by L'Garde, Inc. and AEC-ABLE Engineering, Inc. to develop scale-model solar sail hardware over the next two years, and to demonstrate its functionality on the ground.[1-3] Both are 4-quadrant, square sail designs with four lightweight diagonal booms (linear density < 100 g/m^2) and ultra-thin membranes (areal density < 10 g/m^2) as shown in Fig. 1. To support this technology, the authors are engaged in a focused research effort to develop an integrated diagnostics instrumentation package capable of accurate monitoring of solar sail structures such as these during ground and near-term flight experiments.

The approach taken focuses on lightweight optical sensing techniques based on photogrammetry to measure solar sail shape and dynamics and thermography to measure its temperature. Some non-optical sensors will also be used including accelerometers, load cells, and thermocouples. The diagnostics package must be low mass (< 10 kg for scale-model sails, evolvable to 2 kg for a 5000 m^2 mission sail) and must measure/monitor key sail structural parameters such as sail support tension, boom and sail deflection, boom and sail natural frequencies, sail temperature, and sail integrity.[4] This paper discusses the following aspects of designing an integrated diagnostics

* Professor and Chair, Mechanical Engineering Department, Senior Member AIAA.
† Graduate Research Assistant, Mechanical Engineering Department.
‡ Senior Research Engineer, Structural Dynamics Branch, Mail Stop 230, Member AIAA.
§ President, Tether Applications, Inc., 1813 Gotham St., Senior Member AIAA.
** Associate Professor, Integrated Science and Technology, MSC 4310, Senior Member AIAA.
†† Associate Professor, Integrated Science and Technology, MSC 4102.
‡‡ Aerospace Engineer, Advanced Optical Systems Development Group, SD71.

system: measurement needs and goals, related aspects of photogrammetry and thermography measurement technologies, and some specific modeling and measurement challenges for solar sails.

II. Measurement Needs and Goals

For the greater part of the history of scientific inquiry, experiment has been the major, and often the sole, source of analysis. There are several important reasons for performing experiments:

- Reliance on an experimental model absent other models
- Provide needed data for theoretical/numerical model computation
- Validate theoretical/numerical modeling methods
- Better illuminate poorly understood phenomena
- Expose completely unknown phenomena

In the present case–the experimental measurement of solar sails–all of these reasons have relevance to one extent or another, as the following examples suggest:

- Reliance on an experimental model absent other models. *Deployment is such a complicated phenomenon, that at least for some solar sail configurations, reliable models may be simply unavailable.*
- Provide needed data for theoretical/numerical model computation. *The need for material property data, such as elastic modulus or optical reflectivity, is a common example.*
- Validate theoretical/numerical modeling methods. *Comparison of model results to experimental data is essential to providing confidence in the predictions for risk reduction.*
- Better illuminate poorly understood phenomena. *Damage evolution such as tear propagation, while understood to some extent on the ground, is poorly understood in the space environment.*
- Expose completely unknown phenomena**.** *It is the unexpected, unasked questions that are perhaps the most serious challenges to risk reduction.*

Among the above, modeling validation is perhaps the most critical to solar sailing success. Given the need to move solar sails to a Technology Readiness Level (TRL) of 7 for flight manifesting, and given the difficulty of ground testing full-scale sails in a relevant environment, it is imperative to have reliable theoretical/numerical models that can provide the critical transition from scale model tests to TRL 7 full scale designs.

The experimental measurements must be considered in the context of high-fidelity computational models of the sail structure. The sails themselves are membrane structures, and as such are delicately constrained, and cannot withstand compressive or transverse loads without some initial prestress. Under sufficient compressive loads to overcome any initial tensile prestress, the membrane wrinkles out of plane. Wrinkling may reduce the propulsive efficiency of a solar sail, may cause hot spots where membrane overheating can occur, and will likely cause significant departure from unwrinkled dynamic response behavior. Furthermore, slack directions and areas in the sail represent load-carrying indeterminacy that needs to be minimized to increase confidence in structural integrity under mission conditions. Because membrane structures change shape in partial response to applied loads, the total response of the sail is complicated and not intuitive. Hence, guidance from structural models in developing the in-space measurement approach is highly desirable.

There are several solar sail modeling methods that need to be evaluated. Relevant field variables predicted by the methods would include:

- Static sail shape
- Center of pressure
- Sail strain
- Lowest several sail natural frequencies and mode shapes
- Static boom shape
- Boom loading
- Lowest several boom natural frequencies and mode shapes

Other important solar sail measurement tasks include:

- Measure sail support tension
- Measure sail temperature
- Measure boom root loads
- Measure boom tip accelerations
- Observe deployment and report both qualitative and quantitative results
- Observe sails, booms, and other mission-critical components for structural health monitoring

It is essential to establish the accuracy of experimental solar sail measurements to avoid both under design and over design of an in-space diagnostics system. At a minimum, the experimental data must be at least as accurate as the models to be validated, although several times more accuracy is desirable for higher confidence. But how accurate will the model predictions be? Consider that a 7 kPa (1 psi) membrane ("skin") stress in a 21 MPa (300 ksi) elastic modulus sail will result in approximately 3 micro-strain, well within the capability of modern finite element (FE) codes. When compared to classical membrane solutions, FE computed frequencies and mode shapes have shown to compare extremely well. Generally, computational model results will be considered successful if they are within 5% - 10% of experimental "truth."

Center of Pressure (CP) is an important parameter in the design and control of solar sails, as is the Center of Mass (CM). CP is the position through which a force that is statically equivalent to the pressure load acts. The CP-CM offset and its uncertainty are fundamental to solar sail guidance and control.[5] The CP in some ways is a metric for sail computation not unlike "rms figure error" is for antennas and optics. The CP depends on the global and local shape of the membrane, and hence sail shape is critical for solar sail model validation. Two methods of CP determination are possible:

1. Synthesis of boundary reaction force components leads to a resultant reaction force vector, which must pass through the CP.
2. Direct integration of pressure loads finds the statically equivalent concentrated load vector, which must pass through the CP.

Given that the reaction force vector directions may not be experimentally measurable (although the reaction magnitudes may be), direct integration of the pressure load over the deformed sail surface may be required. To date, most solar sail CP analyses in the public domain have considered only a flat (non-billowed) sail. See for example Ref. 6. To illustrate the importance of not ignoring the sail billow in the CP calculation, consider a curve y = f(x) as defined in Fig. 2.

Let **t** and **n** be unit vectors tangential and normal to the curve, respectively, and the unit vectors in the x and y coordinate directions be given by **i** and **j**, respectively. In the direct integration method for Center of Pressure, an integral with features such as the following occurs:

$$\int_0^L \mathbf{j}\bullet\mathbf{t}\,ds$$
$$ds = \sqrt{1+(y')^2}\,dx, \qquad y' = \frac{dy}{dx} \tag{1}$$
$$d\mathbf{s} = dx\mathbf{i} + dy\mathbf{j} \Rightarrow d\hat{\mathbf{s}} = \ldots = \frac{\mathbf{i} + y'\mathbf{j}}{\sqrt{1+(y')^2}} = \mathbf{t}$$

If the curve is flat (y = constant), then the integral (1) is trivially zero. However, if the curve is, for example, parabolic and of the form $y = y_0(x/a)^2$, then

$$\int_0^L \mathbf{j}\bullet\mathbf{t}\,ds = \int_0^a y'dx = \ldots = y_0 \tag{2}$$

In this case, the error in ignoring the sail billow is of the order of the sag y_0 itself; sag on a large solar sail could easily be on the order of one meter or more.

The study of vibrating membranes goes back at least three centuries.[7] Motivations for such studies were the solution of practical problems; a rich example is the investigation of acoustics of musical instruments such as drums and bells. In modern times, membranes have provided a canonical formalism for mathematical analysis due to their vanishing thinness and resultant absence of any bending rigidity. However, numerous practical applications exist for membrane structures, and are in fact growing in importance. Examples include architectural and civil structures, diaphragms in switches and transducers, biomedical prostheses such as artificial arteries and organs, and space-based applications such as radio antennas, optical reflectors, and solar sails. Development of attitude control systems for solar sails will require good knowledge of the vibrational response characteristics of these large and highly compliant structures.

Dozens of theoretical studies of membrane vibrations exist in the literature. These studies cover linear and nonlinear models, various shapes and boundary configurations, and numerous analysis methods including closed-form, asymptotic expansions, and numerical methods (FEM, BEM, etc.). Such studies are ongoing and of current interest. However, probably less than a dozen experimental studies can be found in the open literature. Even the simplest classical cases have not been thoroughly investigated. This is due at least in part to the extreme flexibility and lightness of membranes and the corresponding requirement for noncontacting measurement methods. What data that does exist is severely limited, inaccessible, or insufficient for validating theoretical results.

Vibration measurements on solar sails are particularly challenging due to the very low frequencies (< 1 Hz) of the first several fundamental modes, extremely large sizes, large stiffness variation between the booms and sails, and modal coupling between boom and sail dynamics, among other problems. Moreover, answers to pressing questions need to be addressed. How do effects like wrinkling, thermal loading, and manufacturing variability affect the vibrational response of membrane/inflatable space structures in general, and solar sails in particular? Can adaptive control methods use vibration information for local and global state estimates in such structures? [8,9]

Table 1 lists the types of measurements needed for validating structural analytical models and modeling techniques of solar sails. Also listed are estimated ranges of the measurement parameters and an accuracy target for each parameter assuming a sail size of 70 meters. Accuracy targets for other sail sizes vary proportionately. This information is based in part on requirements listed for a proposed New Millennium Program ST7 solar sail flight experiment.[10] Note that the desired measurement parameters contain two stress quantities. There are no known methods to directly measure stress in structures (stress itself is a hypothesized concept--see Cauchy's Stress Hypothesis in Ref. 11). Stress is always derived indirectly from directly measured quantities, typically kinematic quantities such as static displacement or strain, or dynamic frequency, damping, and phase. These kinematic quantities are then coupled with a model, such as material constitutive relations, to derive the associated stress. For an in-space measurement system, an attractive noncontacting method for measuring the desired kinematic quantities of sail shape (displacement) and sail dynamics (frequency, damping, mode shapes) is photogrammetry, discussed next.

III. Photogrammetry Measurements

Photogrammetry is the science of measuring the location and size of three-dimensional (3D) objects using photographs.[12] The image analysis procedures are related to those used in surveying. When dealing with time sequences of images, this technology is often called "videogrammetry" (or "videometrics") instead of "photogrammetry," although either term is acceptable.[13] Modern close-range photogrammetry uses digital imaging sensors (either CCD or CMOS) and computer data analysis and is capable of measuring hundreds or thousands of object points simultaneously. Measured sets of object points, also known as "point clouds," characterize the static shape of engineering structures. Using sequences of images, they characterize the corresponding structural dynamic (i.e., vibration) properties as well. For in-space solar sail application, a set of video cameras designed for photogrammetry measurements of sail shape and dynamics would also provide rich data sets for both qualitative viewing of the sail and health monitoring purposes.

Digital photogrammetry records the object from at least two camera positions and provides numerical data in the form of 3D coordinates of discrete points on the surface of the object. These discrete points can be natural surface

features; however, when high accuracies are required, natural features can be inadequate. Solid-colored circular targets are installed (if possible) in these situations. Rigorous statistical analysis is used in the numerical processing so that the 3D coordinates are accompanied by their covariance matrix and other statistics that indicate the accuracy, precision, and reliability of the data. Such information is necessary when spatial deformation is indicated by the difference between sets of coordinates obtained at discrete epochs (instants of time), enabling decisions to be made at specific levels of confidence about what difference, if any, is caused by a change in the measured object. The photogrammetric technique is extremely flexible, able to acquire measurements simultaneously over the surfaces of large objects, and has been proven through its successful application to monitoring spatial deformation of a wide range of structures, including various gossamer research structures.[14]

In practice, the measurement accuracy achieved with photogrammetry is highly dependent on several mutually dependent factors, including:

- Size and geometry of the test structure
- Number of cameras and their image resolution
- Camera synchronization (for dynamics measurements)
- Locations and pointing directions of cameras
- Illumination conditions
- Clarity and contrast of surface features (targets)
- Camera and lens characteristics
- Image compression procedures
- Camera stability
- Calibration and data analysis procedures

Numerical simulations were conducted to calculate the expected photogrammetric measurement precision of various assumed camera geometries for a square solar sail structure. Figure 3 shows the selected configurations. Each symbol in Fig. 3 indicates the location of one or more cameras, as noted. Each camera used an imaging sensor with 1024 x 1024 pixels, and the assumed target marking (centroiding) precision was 0.5 pixels. Figure 4 shows the corresponding results for in-plane measurement precision, out-of-plane measurement precision, and total mean measurement precision. Each bar in Fig. 4 is scaled relative to the maximum value obtained, which is the in-plane result for camera configuration 2A. Note that more-precise measurements (i.e., better measurements) correspond to smaller bars in these plots. As expected, camera configuration 3 has the best measurement precisions, but of course this design is the most difficult to implement of those studied since it requires a camera mast at the tip of each sail boom, which may be unacceptable for a flight vehicle. The second-best measurement configuration of those studied is No. 1, which uses a stereo pair of camera clusters on an offset, horizontal connecting bar.

IV. Thermography Measurements

Measuring solar sail temperatures with infrared (IR) cameras is also being investigated. This technology, known as infrared thermography, does have limitations however that must be considered. The two most important ones are: 1) an IR detector array must be kept cool, even to cryogenic levels for some types, and 2) a detector array cannot distinguish between emitted and reflected photons, which is a significant problem if the reflected component is unpredictable or is much greater than the emitted. These limitations are minimized if temperature profiles are obtained from the back side of the solar sail (i.e., from the side of the sail facing away from the sun).

There are several advantages to locating the thermal imager on the back side of the spacecraft. The imager would be in the shadow of the sail and direct solar heating would be avoided. Without a large solar heat load it may be possible to passively cool the detector array. The imager would still detect photons from space (or from Earth albedo radiation) that are reflected from the back surface of the sail. However, the reflected photons would be at a lower energy state than those emitted from the sail surface because the temperature of space is lower than that of the sail. (Unless the sail is quite close to a planet, moon, or asteroid, there will generally be far too little infrared energy incident on the back of the sail to perturb measurements of the back-side thermal emissions.) Reflected long-wave planetary radiation may be an issue in low orbit, but not when the sail is far from a planet or moon. Therefore, the reflected component of the energy incident on the detector array can generally be characterized and accounted for

during conversion of the raw infrared data to temperature. There may also be a small component of energy transmitted through the sail that needs to be accounted for.

Sail temperature measurements will provide information on the performance of membrane coatings. Additionally, knowledge of the temperature field and associated thermal strain distribution are important for predicting and understanding in-space membrane stresses and membrane dynamics. Membrane stresses created by mechanical pre-tensioning may be low, for example, < 70 kPa (10 psi). Small temperature gradients across the sail surface can create thermal strains that exceed these mechanical strains. Blandino et al. experimentally demonstrated the effect of temperature gradients on a spot-heated membrane.[15] A 50 ˚C temperature gradient was created in the center of the membrane. Outside the heated region the membrane remained near ambient temperature because conduction across the membrane is minimal. Thus, thermal expansion occurred mostly in the heated region, causing a significant, localized slack area. Corresponding effects of this phenomenon on sail dynamics has not yet been investigated.

To better understand the temperature distribution that a solar sail may experience in space, a thermal model was developed. The sail was modeled using square elements. Figure 5 shows the radiation from the sun and interactions with deep space acting on one element. Radiation exchange between elements is neglected since the view factors are infinitesimal. Conduction through the membrane is also neglected. Optical property values are assumed uniform across the membrane and are based on data acquired from a test sample. An expression for the temperature at any point on the sail surface is obtained by performing an energy balance on the sail. The expression for temperature is:

$$T_s = \sqrt[4]{\frac{\alpha_f \dot{q} \cos\phi \cos\theta}{\sigma(\varepsilon_f \varepsilon_b)} + T_\infty^4} \tag{3}$$

where T_∞ is the background temperature, α_f is the front side absorptivity, ε is the emissivity (front and back), σ is the Stefan-Boltzman constant, and $\dot{q}$ is the solar flux. This is essentially the same expression presented by Salama et al.[16] Clearly, the solar flux $\dot{q}$ varies with sail orientation to the sun, but it also varies with billowing of the sail from solar pressure. To approximate the shape of a sail in space, the gravity sag of one quadrant of a 2 m scale model was measuring using photogrammetry. The measured shape is shown in Fig. 6. Although the gravity sag is much greater than the billow due to light pressure in space, the data shown in Fig. 6 can be scaled in the x, y, and z dimensions. Thus it can be used to approximate any sail size and billow depth.

A 40 m x 40 m sail located 1 AU from the sun was considered. The temperature distribution was obtained for angles to the sun of 0˚, 22.5˚, and 45˚ and billow depths of 0, 0.2, and 1 m. The sail material was assumed to be Kapton aluminized on one side (front), and values of α_f, ε_f, and ε_b were taken as 0.09, 0.04 and 0.50, respectively. Table 2 shows the average sail temperature and difference between maximum and minimum temperatures, ΔT, for various sail angles and billow depths. Although the temperature differences seem small, to understand their significance they must be used to determine the magnitude of the resulting thermal strains. The thermal strains must then be compared to the mechanical strains. Table 3 shows the coefficient of thermal expansion for three candidate sail materials and the resulting thermal strain due to temperature differences. To compare the mechanical and thermal strains, Table 4 lists corresponding strains due to a 70 kPa (10 psi) mechanical load. For both Kapton and Mylar, the thermal strain exceeds the mechanical strain when the temperature gradient is approximately 1.2 ˚C. For CP1, the thermal strain exceeds the mechanical strain when the temperature gradient is less than 0.5 ˚C. If the sail membrane is subjected to loads smaller than 70 kPa, then the temperature gradients required for the thermal strain to exceed the mechanical strain will reduce accordingly.

Temperature gradients across the sail surface can develop from variations in metallic coatings, sail orientation to the sun, and the billowed shape of the sail. The simple model presented above illustrates that only small temperature gradients, on the order of 1 ˚C, are necessary for the thermal strains to exceed mechanical strains. Consequently, their effect on sail membrane stresses and dynamics can be significant.

V. Other Modeling and Measurement Challenges

Cables that collect loads from the sail membrane quadrants and carry them to the booms complicate the structural configuration of the sail. The cables and membranes carry tensile loads, while the booms carry compressive loads and some bending. Boom loads are likely to be small (perhaps only a few newtons), as are boom deflections. Sail loads are also likely to be small, but deflections may be considerably larger than those of the booms due to the relative differences in stiffness. This wide range of stiffness, coupled with potentially large sail displacements and nonlinear material behavior, provides for challenges in predicting sail response. Boundary conditions are always difficult to know with certainty in any complicated structure. The dynamic response of membranes, due to their no-compression/wrinkling character, is extremely challenging to accurately predict. This implies that, even under the best situations, any sail diagnostics measurement package must be designed to work with considerable uncertainty with respect to structural model predictions.

An important factor in the design of a sun-side photogrammetric measurement system viewing the entire sail is reflected glare and glints from the sail. In most cases, at least one imager will see an intense specular reflection of the sun. Over much of the rest of the sail, wrinkles and creases can cause local specular reflections to the imagers. The glinting width of these features will generally be <<1 pixel, so the brightness seen by the imager will be far less than that of the light source. Full glare can be ~60,000 times brighter than a diffuse-white photogrammetry target, while the diffuse reflection from a non-glinting sail is only ~2% as bright as a target. Therefore, even "micro-glint" can impede image analysis. The brightness of the specular reflection of the sun will be ~85% of full sunlight, due to the imperfect specular reflectivity of the membrane. However, the sail will generally have some local curvature. If the membrane is concave in the region of the specular reflection, the "sunspot" focused onto the imager may be larger and may involve several times more energy than in a direct image of the sun through the same lens. The camera systems must be designed accordingly to handle the worst-case brightness condition.

"Glint" is here used to refer to specular reflection from local creases, wrinkles, or other regions smaller than a pixel (on the camera imager) in at least one direction. This can result in pixel brightness anywhere in the ~3,000,000:1 brightness range between the full intensity of a specular reflection and the diffuse brightness of the sail. Glint should not be a significant problem if membranes are under enough biaxial tension to remove stowage creases and prevent wrinkles (which occur under uniaxial tension). In "suitably tensioned" sails, only seam and edge imperfections are likely to cause significant glint, and keeping photogrammetry targets far enough away from such features can prevent image-analysis problems. However, if the sail membrane tension is kept low during and after deployment, creases from stowage may never fully straighten out. This may cause the glint level to be quite high, and variable across the sail. It seems unlikely that ultra-thin membranes will form creases only at the intended folds when flight-size quadrants of several thousands of square meters are folded. Pleats will probably form in random locations, especially when the once-folded sail is folded again, at right angles to the initial folds, for stowage in the launch container.

In summary, glare and glint are important design considerations for a solar sail photogrammetric measurement system for several reasons, including:

- Potential permanent sensor damage from focused sunlight
- Partial or total loss of useful imaging when glare is too strong
- Difficulty finding and centroiding targets and other features when glint is highly variable
- Difficulty in evaluating long-term changes in diffuse reflectivity if glint is significant
- And also one positive aspect of glint: glint variations may themselves have diagnostic utility

VI. Conclusion

Solar sails are currently undergoing significant development. Interest is high since there are a number of important missions that will be enabled by successful solar sail technology. Solar sails will be large and ultra-lightweight, with high structural compliance, leading to significant challenges in ground testing full-scale sails. Therefore, validated computational models of sail performance will be critical for success. This paper has outlined many of the challenges and opportunities for making the kinds of measurements that would be useful in validating

solar sail structural models, both on the ground and in space. Moreover, such a measurement system would also find important use in sail mission support, particularly in the area of structural health monitoring.

Acknowledgments

The authors express their appreciation to Doug Caldwell and Scott Van Essen of Ecliptic Enterprises Corporation and to Tom Pollock, Diane Hurtado, and Mike Jacox of Texas A&M University for their technical contributions to this activity. Thanks also to Mr. Edward E. Montgomery of the Solar Sail Propulsion project office at NASA Marshall Space Flight Center for sponsoring this work under Phase 1 of the Optical Diagnostic System (ODS) for Solar Sails project.

References

[1]Garbe, G. and Montgomery, E. E., "An Overview of NASA's Solar Sail Propulsion Project," *AIAA Joint Propulsion Conference*, AIAA paper 2003-5274, July 2003.

[2]Lichodziejewski, D. et al., "Bringing an Effective Solar Sail Design Toward TRL 6," *AIAA Joint Propulsion Conference*, AIAA paper 2003-4659, July 2003.

[3]Murphy, D. M., Murphey, T. W., and Gierow, P. A., "Scalable Solar Sail Subsystem," *AIAA Structures, Structural Dynamics, and Materials Conference*, AIAA paper 2002-1703, April 2002.

[4]Proposal Information Package for the In-Space Propulsion Technologies, Cycle 2 ROSS 2002 NRA Amendment, Website: http://www.spacetransportation.com/code_s/ISPT_PIP2003final.pdf, September 2002, p. 14.

[5]Wie, B., "Dynamic Modeling and Attitude Control of Solar Sail Spacecraft," Final Report, JPL Contract No. 1228156, January 2002.

[6]McInnes, C. R., *Solar Sailing: Technology Dynamics and Mission Applications*, Springer-Verlag, London, 1999.

[7]Rayleigh, J. W. S., *The Theory of Sound*, vol. 1, originally published in 1894, Dover Publications Reprint, 1945.

[8]Jenkins, C. H., Kalanovic, V. D., Padmanabhan, K., and Faisal, S. M., "Intelligent Shape Control for Precision Membrane Antennae and Reflectors in Space," *Smart Materials and Structures,* Vol. 8, 1999, pp. 1-11.

[9]Jenkins, C. H. and Tampi, M., "Local Membrane Vibrations and Inflatable Space Structures," *Space 2000*, Albuquerque, NM, 2000.

[10]Price, H., "Solar Sail Technology NMP ST7 Opportunity," Website: http://nmp.jpl.nasa.gov/st7/ST7_TA_Solar_Sail.pdf, May 2001, p. 13.

[11]Jenkins, C. H., Schur, W. W., and Greschik, G., "Mechanics of Membrane Structures," Chapter 3 in Jenkins, C.H. (Editor), *Gossamer Spacecraft: Membrane/Inflatable Structure Technology for Space Applications*, AIAA Progress in Astronautics and Aeronautics Series, vol. 191, 2001.

[12]Atkinson, K. B. (editor), *Close Range Photogrammetry and Machine Vision*, Whittles Publishing Company, 2001.

[13]El-Hakim, S. F. (editor), *Videometrics and Optical Methods for 3D Shape Measurement*, SPIE Proceedings No. 4309, January 2001.

[14]Pappa R. S. et al., "Photogrammetry Methodology Development for Gossamer Spacecraft Structures," *Sound and Vibration*, Vol. 36, No. 8, August 2002, pp. 12-21.

[15]Blandino, J. R. et al., "The Effect of Asymmetric Mechanical and Thermal Loading on Membrane Wrinkling," *AIAA Structures, Structural Dynamics, and Materials Conference*, AIAA paper 2002-1371, April 2002.

[16]Salama, M., McInnes, C., and Mulligan, P., "Gossamer Sailcraft Technology," Chapter 19 in Jenkins, C. H. (editor), *Gossamer Spacecraft: Membrane/Inflatable Structure Technology for Space Applications*, AIAA Progress in Astronautics and Aeronautics Series, vol. 191, 2001.

Table 1: Measurement goals for a 70 m solar sail flight experiment.
(Based partly on Ref. 10)

Parameter	Expected Range of Values	Accuracy Target	Notes
Deployment Dynamics	*Qualitative:* Video coverage of entire deploying sail *Quantitative:* Measure trajectories of the deploying booms & membranes	Qualitative: High-quality video at 10+ frames per second Quantitative: 40 mm	This data is measured only once, so cameras for this purpose can be located off the sailcraft (e.g., on a carrier platform) or ejected afterwards to minimize mass.
Deployed Shape	0 to 2 m (est.) from planarity	20 mm	20 mm is the mean accuracy for a uniformly distributed grid of targets.
Deployed Vibration Characteristics	Natural Frequencies: First 10 system modes < 1 Hz Damping: < 2% Amplitudes: < 1 m	Natural Frequencies: Within 1% Damping: Within 10% Amplitudes: 20 mm	Image frame rate of cameras at least 2x the highest vibration frequency of interest.
Sail Support Tension	0 to 50 N	0.1 N	Will investigate in-situ measurement possibilities with L'Garde & ABLE.
Boom Stress	Deployment: 0 - 15 x 10^6 Pa Operational: < 1 x 10^6 Pa	Deployment: 10^5 Pa Operational: 10^4 Pa	Highest stress levels occur during deployment, but difficult to measure then. Operational stresses much lower and also difficult to measure directly.
Sail Film Stress	0 - 10^6 Pa (Mostly under 10^5 Pa)	10^3 Pa	Very low operational stresses. Can be estimated using measured wrinkle patterns, sail shape, modes, and predictive structural model.
Sail Temperature	Full-field measurement with IR camera (thermography)	10 deg C	Important for some solar sail missions, particularly in the inner solar system.
Sail Integrity	Identified by data trends versus time and/or direct optical observation	High-resolution imagery, perhaps on one sail quadrant only	If not mass-prohibitive, high-resolution camera will include pan/tilt/zoom capability.

Table 2: Sail temperature for various sun angles and billow depths.

	Sun-Sail Angle					
Billow Depth	**0°**		**22.5°**		**45°**	
0.0 m	-21.9 °C	0.0 °C	-26.6 °C	0.0 °C	-42.7 °C	0.0 °C
0.2 m	-21.9 °C	0.2 °C	-26.8 °C	0.5 °C	-43.3 °C	1.0 °C
1.0 m	-21.9 °C	0.3 °C	-27.9 °C	2.3 °C	-45.7 °C	5.2 °C
	T_{avg}	**ΔT**	**T_{avg}**	**ΔT**	**T_{avg}**	**ΔT**

Table 3: Membrane thermal strains for three candidate materials.

Material	Coefficient of Thermal Expansion	ΔT	$\varepsilon_{thermal}$
Kapton	2.0×10^{-5} / °C	0.2 °C	4.0 με
		0.5 °C	10.0 με
		1.5 °C	30.0 με
		2.5 °C	50.0 με
		5.0 °C	100.0 με
Mylar	1.7×10^{-5} / °C	0.2 °C	3.4 με
		0.5 °C	8.5 με
		1.5 °C	25.5 με
		2.5 °C	42.5 με
		5.0 °C	85.0 με
CP1	3.7×10^{-5} / °C	0.2 °C	7.4 με
		0.5 °C	18.5 με
		1.5 °C	55.5 με
		2.5 °C	92.5 με
		5.0 °C	185.0 με

Table 4: Membrane mechanical strains for a tension loading of 70 kPa (10 psi).

Material	Tensile Modulus	$\varepsilon_{mechanical}$
Kapton	2.96×10^{9} Pa	23.2 με
Mylar	3.79×10^{9} Pa	18.2 με
CP1	4.20×10^{9} Pa	16.4 με

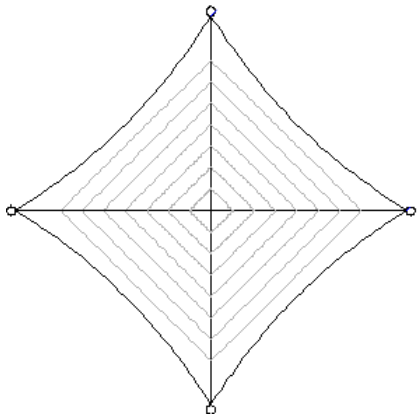

a) L'Garde sail design with boom tip attitude-control vanes

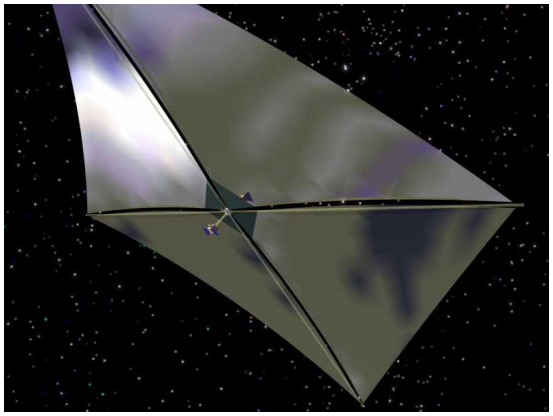

b) AEC-ABLE sail design with articulating attitude-control mast

Figure 1: Solar sail concepts selected for further development by NASA's ISP program.

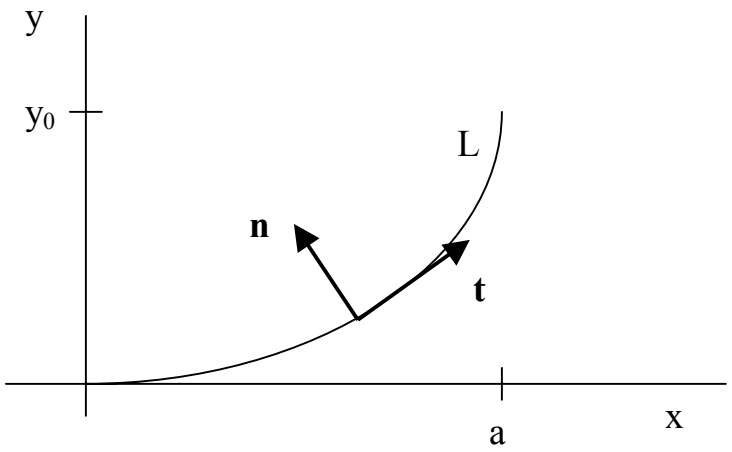

Figure 2: Illustrative sail curvature example.

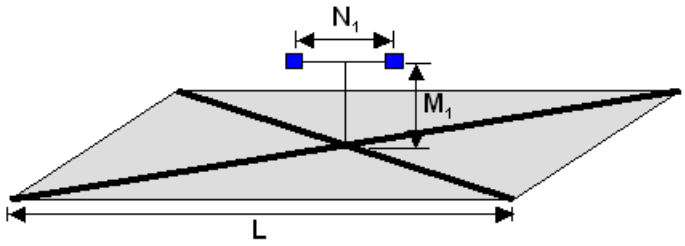

Eight 45-deg cameras at each location

- $M_1 = 0.25L$
- $N_1 = 0.5M_1$

a) Camera Configuration No. 1

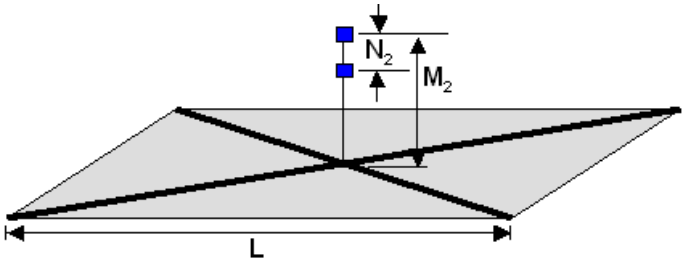

Four 90-deg cameras at each location

Config. 2A:
- $M_2 = 0.4L$
- $N_2 = 0.25M_2$

Config. 2B:
- $M_2 = L$
- $N_2 = 0.25M_2$

b) Camera Configuration No. 2

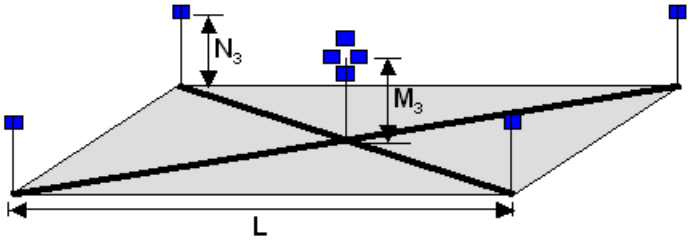

One 90-deg camera (or camera cluster) at each location

- $M_3 = 0.1L$
- $N_3 = M_3$

c) Camera Configuration No. 3

Front and back cameras see same targets

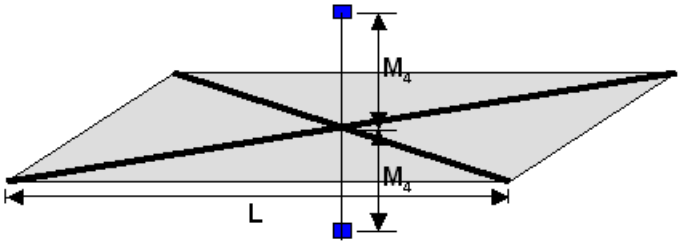

Four 90-deg cameras at each location

Config. 4A:
- $M_4 = 0.25L$

Config. 4B:
- $M_4 = 0.5L$

d) Camera Configuration No. 4

Figure 3: Candidate camera configurations for photogrammetry. Symbols show camera locations.

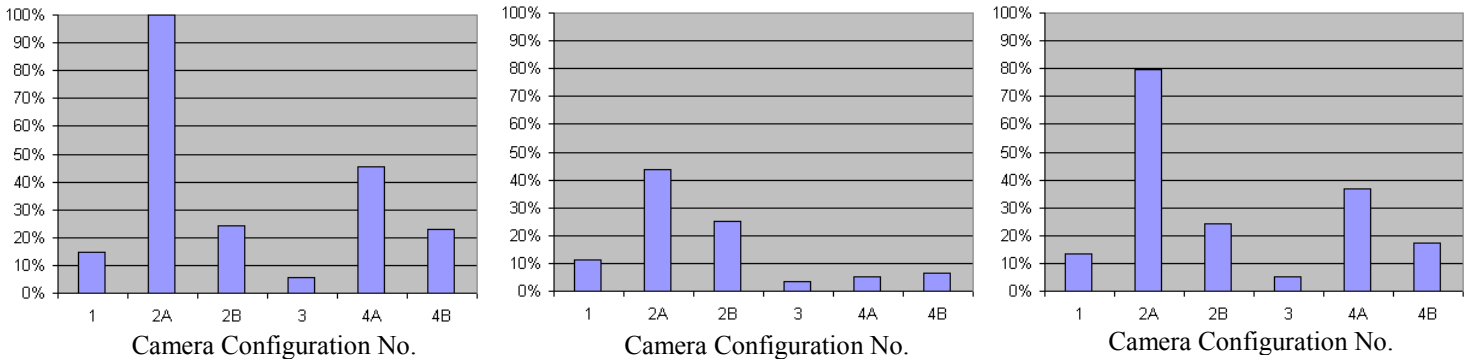

a) In-plane precision **b) Out-of-plane precision** **c) Total mean precision**

Figure 4: Relative photogrammetric measurement precisions for candidate camera configurations. (Smaller is better.)

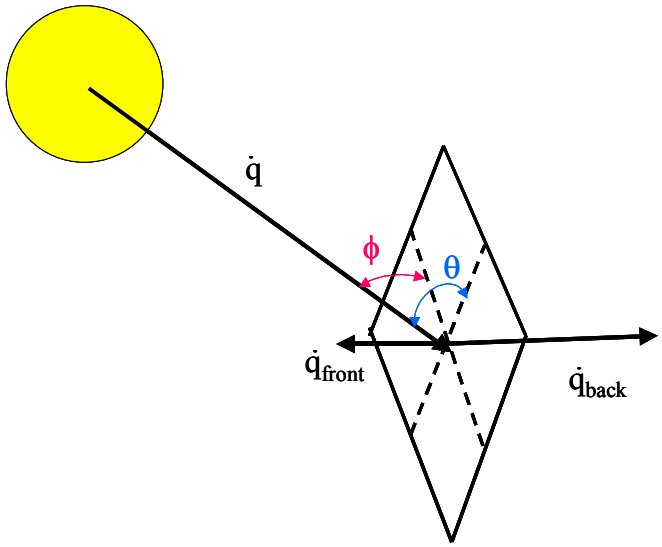

Figure 5: Radiation interactions for a sail element.

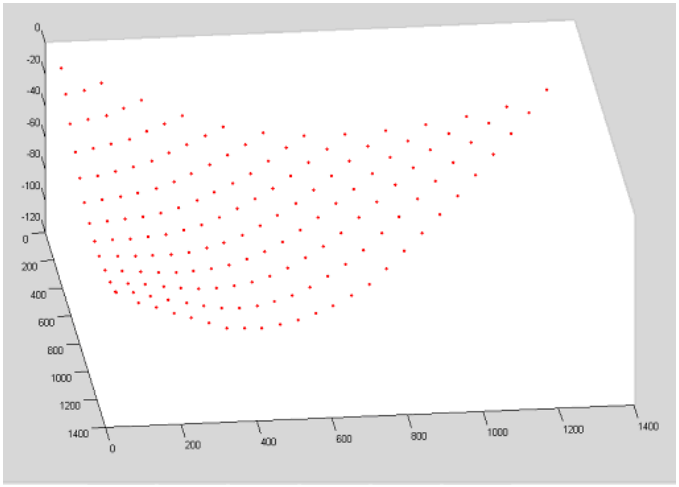

Figure 6: Gravity sag shape used to approximate light pressure billow of solar sail.